Electronic Supplementary Information for Dalton Transactions

Electronic Supplementary Information for

Spin Canting and/or Metamagnetic Behaviors of Four Isostructural Grid-Type Coordination Networks

Xiao-Ning Cheng,[a,b] Wei Xue,[a] Jun-Hou Huang[a] and Xiao-Ming Chen*[,a]

[a]*MOE Laboratory of Bioinorganic and Synthetic Chemistry / State Key Laboratory of Optoelectronic Materials and Technologies, School of Chemistry and Chemical Engineering, Sun Yat-Sen University, Guangzhou 510275, China*

[b] *Instrumental Analysis and Research Center, Sun Yat-Sen University, Guangzhou 510275, China*

Fax: +86-20-84112245; Tel: +86-20-84112074

e-mail: cxm@mail.sysu.edu.cn (X.-M. Chen)

Table S1. Selected bond lengths (Å) and bond angles (°) in **1·Co**, **2·Co and 2·Mn**.

1·Co		**2·Co**		**2·Mn**	
Co(1)-O(5)#1	2.030(2)	Co(1)-O(4)#1	2.001(3)	Mn(1)-O(5)#1	2.077(2)
Co(1)-O(4)	2.092(2)	Co(1)-O(3)	2.083(3)	Mn(1)-O(2)	2.147(2)
Co(1)-O(3)	2.103(2)	Co(1)-O(5)	2.098(3)	Mn(1)-O(4)	2.162(2)
Co(1)-O(2)#2	2.126(2)	Co(1)-N(1)	2.135(3)	Mn(1)-O(3)#2	2.226(2)
Co(1)-N(1)	2.146(2)	Co(1)-O(1)	2.180(3)	Mn(1)-N(1)	2.248(2)
Co(1)-O(1)	2.152(2)	Co(1)-O(2)#2	2.199(3)	Mn(1)-O(1)	2.295(2)
O(5)#1-Co(1)-O(4)	94.82(8)	O(4)#1-Co(1)-O(3)	97.6(1)	O(5)#1-Mn(1)-O(2)	99.57(7)
O(5)#1-Co(1)-O(3)	95.92(7)	O(4)#1-Co(1)-O(5)	99.8 (1)	O(5)#1-Mn(1)-O(4)	99.41(7)
O(4)-Co(1)-O(3)	91.59(7)	O(3)-Co(1)-O(5)	92.1(1)	O(2)-Mn(1)-O(4)	91.57(7)
O(5)#1-Co(1)-O(2)#2	90.34(7)	O(4)#1-Co(1)-N(1)	113.3(1)	O(5)#1-Mn(1)-O(3)#2	86.81(7)
O(4)-Co(1)-O(2)#2	174.22(6)	O(3)-Co(1)-N(1)	147.5(1)	O(2)-Mn(1)-O(3)#2	89.27(7)
O(3)-Co(1)-O(2)#2	90.47(7)	O(5)-Co(1)-N(1)	92.2(1)	O(4)-Mn(1)-O(3)#2	173.49(7)
O(5)#1-Co(1)-N(1)	115.47(8)	O(4)#1-Co(1)-O(1)	170.5(1)	O(5)#1-Mn(1)-N(1)	117.67(8)
O(4)-Co(1)-N(1)	89.81(7)	O(3)-Co(1)-O(1)	73.8(1)	O(2)-Mn(1)-N(1)	141.22(7)
O(3)-Co(1)-N(1)	148.35(7)	O(5)-Co(1)-O(1)	84.8(1)	O(4)-Mn(1)-N(1)	92.55(6)
O(2)#2-Co(1)-N(1)	85.61(7)	N(1)-Co(1)-O(1)	74.5(1)	O(3)#2-Mn(1)-N(1)	82.78(6)
O(5)#1-Co(1)-O(1)	169.90(7)	O(4)#1-Co(1)-O(2)#2	86.0(1)	O(5)#1-Mn(1)-O(1)	168.87(7)
O(4)-Co(1)-O(1)	85.21(7)	O(3)-Co(1)-O(2)#2	89.6(1)	O(2)-Mn(1)-O(1)	70.97(6)
O(3)-Co(1)-O(1)	73.99(6)	O(5)-Co(1)-O(2)#2	173.7(1)	O(4)-Mn(1)-O(1)	86.97(7)
O(2)#2-Co(1)-O(1)	90.17(7)	N(1)-Co(1)-O(2)#2	83.1 (1)	O(3)#2-Mn(1)-O(1)	87.20(7)
N(1)-Co(1)-O(1)	74.62(7)	O(1)-Co(1)-O(2)#2	89.8 (1)	N(1)-Mn(1)-O(1)	70.78(6)
#1 -x+3/2,y+1/2,z; #2 -x+1,y+1/2,-z+3/2		#1 -x-1/2,y,z+1/2; #2 -x-1,-y,z+1/2		#1 -x-1/2,y,z+1/2; #2 -x-1,-y-1,z+1/2	

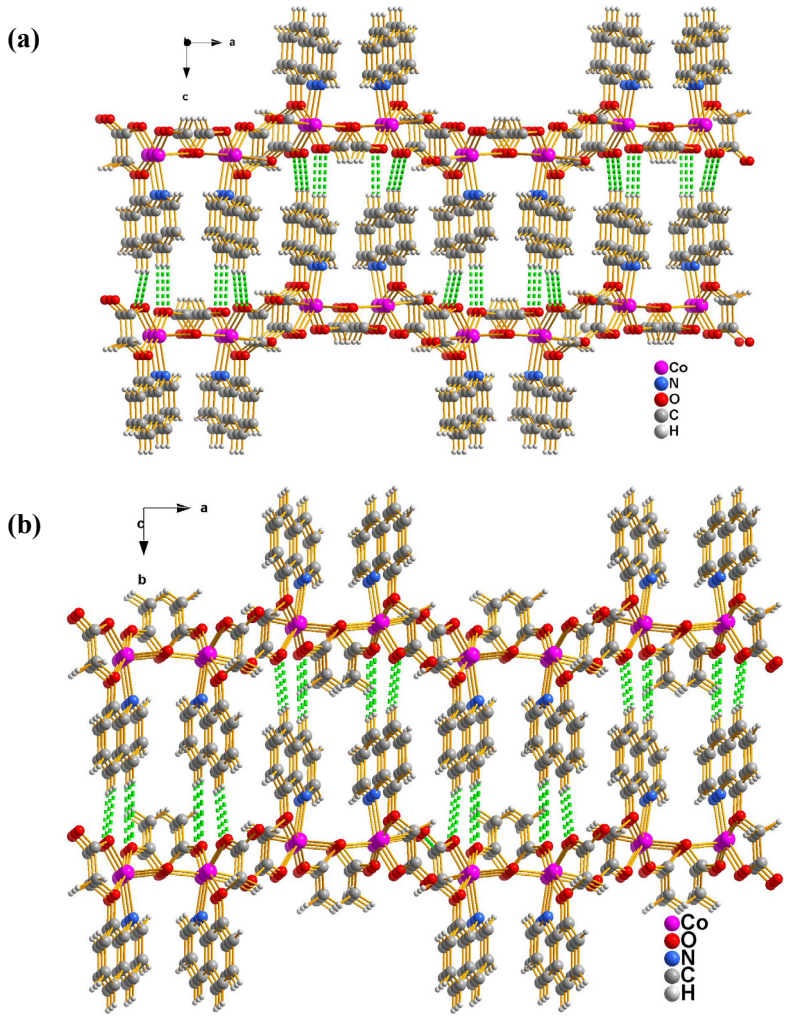

Figure S1. Side views of 3D packing structures of **1·Co** (a) and **2·Co** (b).

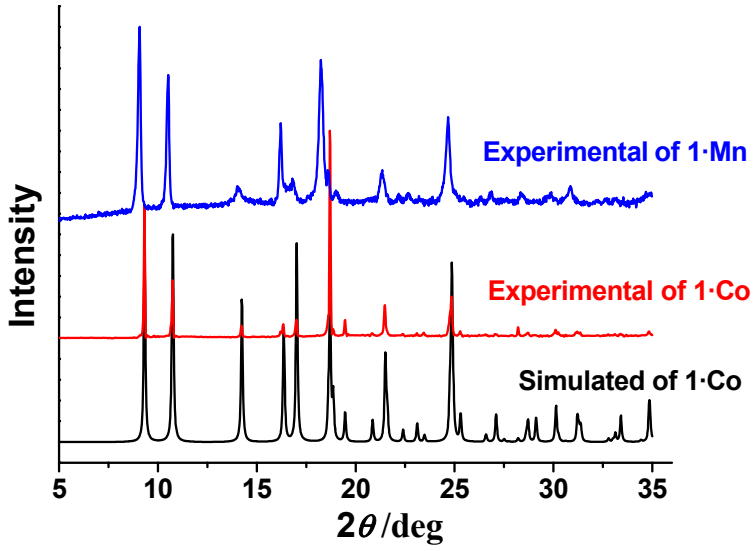

Figure S2. The simulated and experimental X-ray powder diffraction patterns of **1·Co** and **1·Mn**.

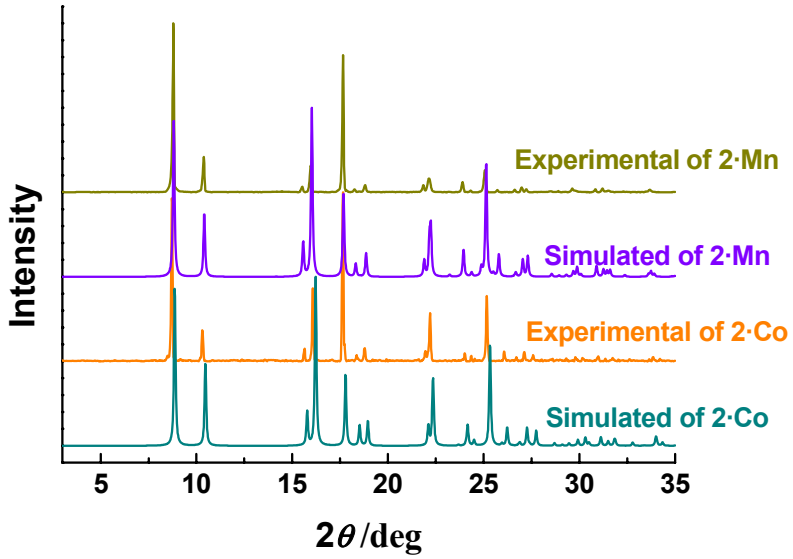

Figure S3. The simulated and experimental powder X-ray diffraction patterns of **2·Mn** and **2·Co**.

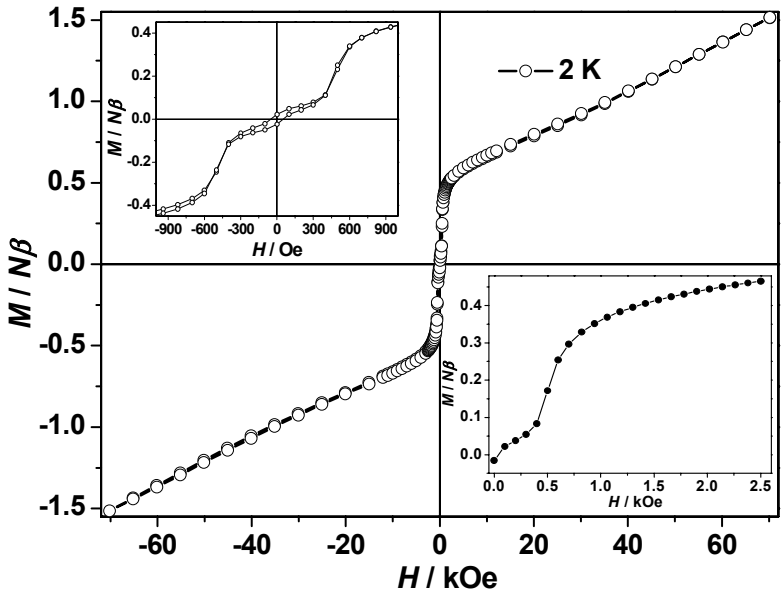

Figure S4. Hysteresis curve for **1·Co** at 2 K. Insets: a blow-up of the hysteresis loop and *M-H* plot in the lower field region.

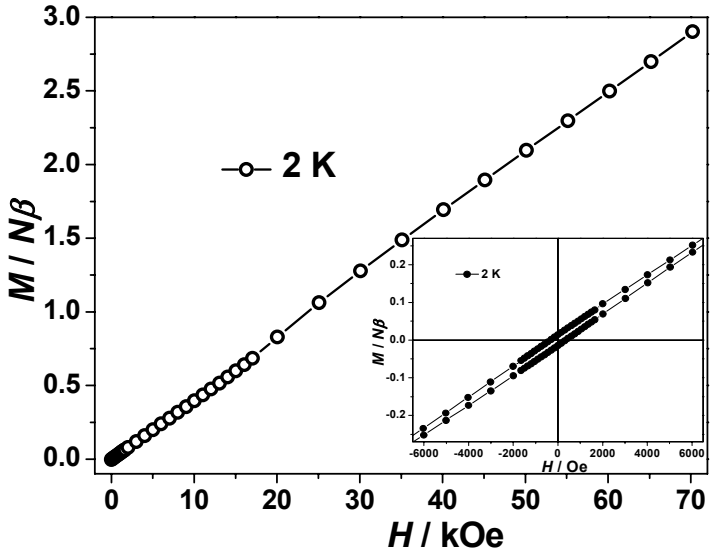

Figure S5. *M-H* plot and the blow-up of hysteresis curve (inset) at 2 K for **1·Mn**.

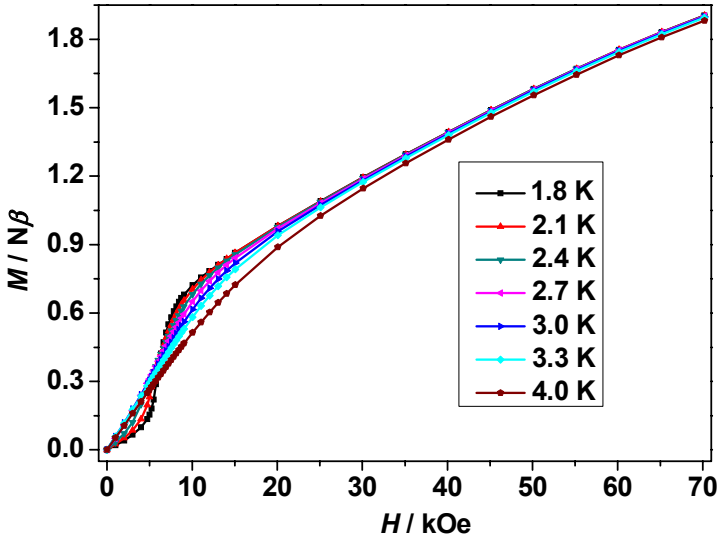

Figure S6. Field-dependence magnetization for **2·Co** at different temperatures.

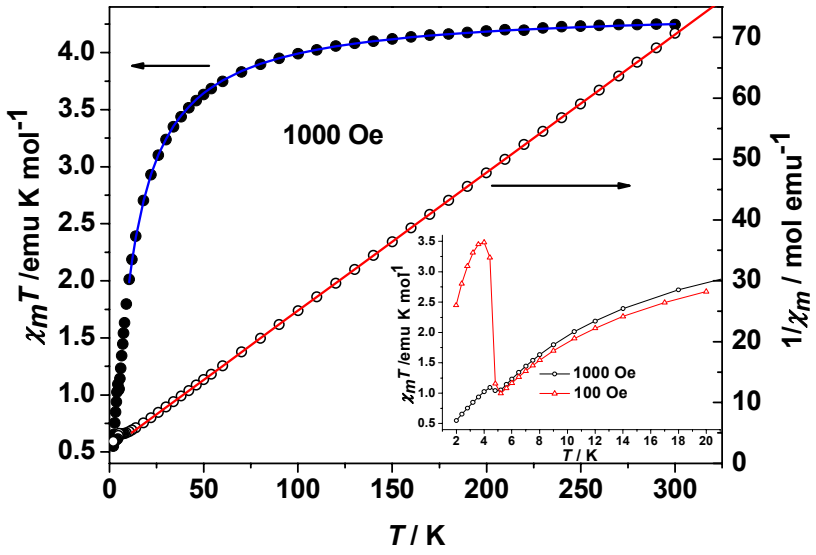

Figure S7. $\chi_m T$–T and $1/\chi$-T plots for **2·Mn** at 1000 Oe. The solid lines represent the best fit of the experimental data to Equation 1 (blue) and Curie-Weiss law (red), respectively. Inset: field-cooled magnetization curves for **2·Mn** at different fields.

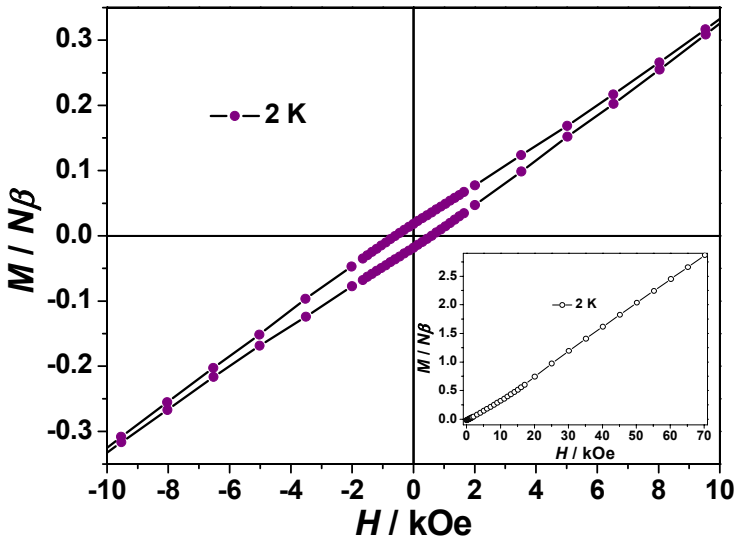

Figure S8. The blow-up of hysteresis curve and *M*-*H* plot (inset) at 2 K for **2·Mn**.